



Irradiation Damage and Semiconducting Properties of $(\text{CdF}_2:\text{Eu})$

Citation

Tzalmona, A. and Peter S. Pershan. 1971. Irradiation damage and semiconducting properties of $(\text{CdF}_2:\text{Eu})$. *Journal of Chemical Physics* 55(10): 4804-4811.

Published Version

doi:10.1063/1.1675582

Permanent link

<http://nrs.harvard.edu/urn-3:HUL.InstRepos:10361958>

Terms of Use

This article was downloaded from Harvard University's DASH repository, and is made available under the terms and conditions applicable to Other Posted Material, as set forth at <http://nrs.harvard.edu/urn-3:HUL.InstRepos:dash.current.terms-of-use#LAA>

Share Your Story

The Harvard community has made this article openly available. Please share how this access benefits you. [Submit a story](#).

[Accessibility](#)

Irradiation Damage and Semiconducting Properties of $\text{CdF}_2:\text{Eu}^*$

A. TZALMONA† AND P. S. PERSHAN

Division of Engineering and Applied Physics, Harvard University, Cambridge, Massachusetts 02138

(Received 11 June 1971)

Thermoluminescence data have been used to unravel the fluorescence spectrum of Eu^{3+} in the insulating CdF_2 host. Optical absorption and EPR measurements of semiconducting $\text{CdF}_2:\text{Eu}$ are the bases of a model of this semiconductor.

I. INTRODUCTION

Cadmium fluoride has the well-known fluorite structure. The series of MeF_2 crystals ($\text{Me}=\text{Cd}, \text{Ca}, \text{Sr}, \text{Ba}$) are easily doped with rare earths. The rare-earth impurity, usually in the trivalent state, substitutes for the divalent cation. The charge compensation needed is usually provided by an interstitial F^- atom. Kingsley and Prener¹ discovered that baking the CdF_2 doped with some rare earths in Cd vapor results in transforming the colorless and insulating crystal into a colored semiconductor. During the process of baking of MeF_2 in the metal vapor, interstitial fluorine atoms are believed to diffuse to the surface, forming MeF_2 with the metal vapor, and for each one molecule two electrons are liberated into the lattice. In the case of $\text{Me}=\text{Ca}, \text{Sr}, \text{Ba}$ the rare earth is converted to the divalent state. In CdF_2 , however, even at low temperatures,³ there is no evidence of most of the rare earth in the divalent state. The difference can most probably be attributed to the greater electron affinity of the Cd^{2+} compared to Ca^{2+} , Sr^{2+} , and Ba^{2+} .⁴ The electrons are located at cadmium sites and form a conduction band. It has been shown by EPR and optical studies that⁵ some of the rare earths represent a "shallow trap" for the conducting electron in the sense that the electron is free to move around the trivalent rare earth on the cadmium sites without converting it to the divalent state.

In $\text{CdF}_2:\text{Eu}$, however, it has been shown⁶ that the converted crystals exhibit Eu^{2+} optical properties. The resistivity of the converted sample is of the order of a few hundred ohm-centimeters compared to a few ohm-centimeters for the shallow traps such as Nd, Sm, Tb, Dy, Ho, Tm. Resistivity measurements show the energy gap of the europium-doped semiconducting CdF_2 is 0.33 eV.⁶

The purpose of the present work is to confirm that Eu^{3+} in CdF_2 represents a deep trap for the electron. We have studied the insulating crystals by means of irradiation damage (thermoluminescence and EPR) and fluorescence; the semiconducting crystal has been studied in terms of optical absorption and EPR. The fluorescence spectrum of Eu^{3+} shows two kinds of local negative charge compensation which result in two different crystal field splittings. The thermoluminescence data are able to separate these two

kinds of Eu^{3+} sites. The converted sample exhibits two absorption bands in the near-infrared region, one is peaked at 2650 cm^{-1} (0.33 eV) and the second at 1100 cm^{-1} (0.136 eV). The EPR measurements show that the electron is indeed trapped at the europium ion which results in a "normal" EPR spectrum of Eu^{2+} . In addition, a broad signal is present at a certain angle⁵ which indicates the existence of exchange interaction between the conducting electron and the paramagnetic Eu^{2+} . This effect disappears at 77°K or lower temperature. On the basis of these experimental results we propose a model to explain the semiconducting properties of $\text{CdF}_2:\text{Eu}$.

II. EXPERIMENTAL RESULTS

A. Irradiation Damage and Fluorescence of Insulating $\text{CdF}_2:\text{Eu}$

Unlike CaF_2 , SrF_2 , and BaF_2 , where the europium ion is embedded in the host mainly as Eu^{2+} , in insulating CdF_2 , only the trivalent state is found in our crystals. The EPR spectrum of our samples at room temperature and liquid nitrogen temperature shows only a small amount of Mn^{2+} [see Fig. 1(a)]. X-ray irradiation of the $\text{CdF}_2:\text{Eu}$ results in partial conversion of Eu^{3+} to Eu^{2+} and a trapped hole in the lattice [see Fig. 1(b)]. Angular variation of the spectrum of a crystal oriented in (100) plane shows that the local symmetry is cubic or very close to cubic. The g factor ($g=1.988$) and crystal field parameters are identical to those reported by Glaser and Glist.⁷ The nature of the hole which accompanies the Eu^{2+} ion has not been established. It is possible that V_K ⁸ centers similar to the V_K centers in CaF_2 , SrF_2 , and BaF_2 exist.⁹ Since the g factor of these hole centers is also close to 2, but their intensity is much weaker than the intensity of the paramagnetic divalent europium, it is not possible to confirm this assumption. The total angular momentum of $\frac{7}{2}$ for Eu^{2+} and $\frac{1}{2}$ for the V_K centers is the reason for the difference in the intensity since the spin magnetization is proportional to $S(S+1)$.

Heating the irradiated sample from 77°K up to 270°K results in gradual disappearance of the EPR spectrum of Eu^{2+} according to Fig. 2(b). A recombination process $\text{Eu}^{2+}+\text{hole}\rightarrow\text{Eu}^{3+}$ occurs which is accompanied with thermoluminescence glow peak at 170°K [Fig. 2(a)]. Such a recombination process,

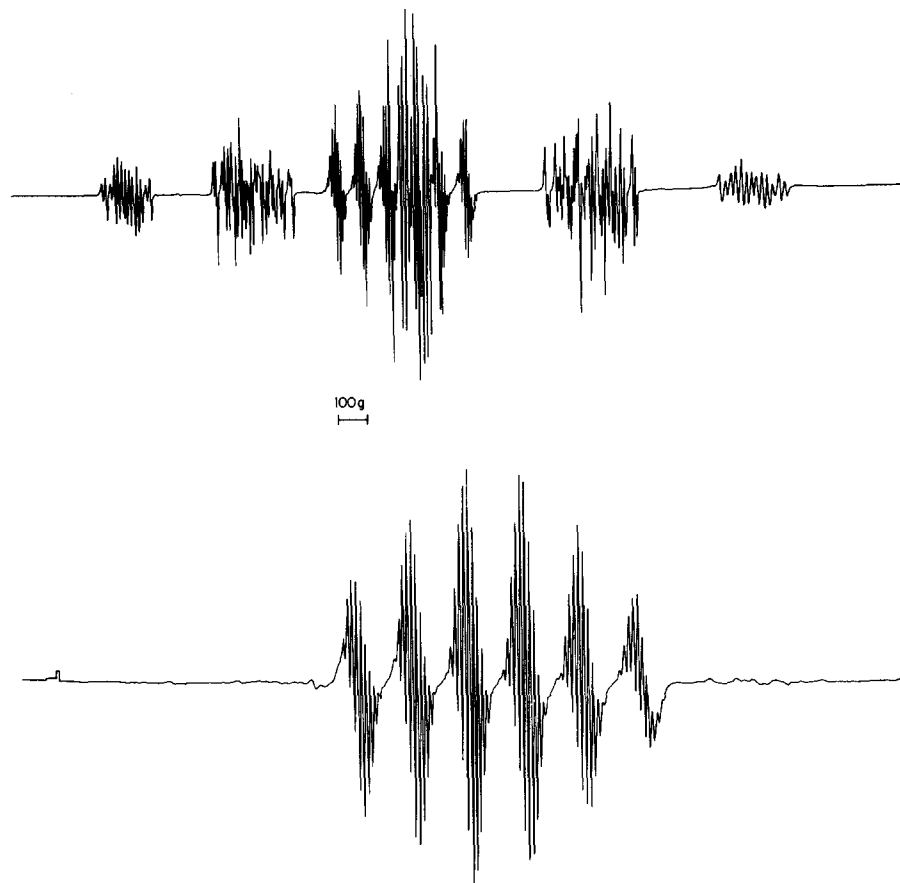


FIG. 1. (a) EPR spectrum around $g=2$ of the irradiated CdF₂:Eu(0.02%). The magnetic field is oriented along the $\langle 100 \rangle$ direction. The seven lines of Eu³⁺ are superposed to the natural impurity of Mn²⁺ in the crystal. (b) Nonirradiated crystal: only Mn²⁺ signal is present.

previously described in detail for CaF₂ host¹⁰ doped with various rare earths, is particularly useful since the spectroscopy of the Eu³⁺ ion is revealed. In Figs. 3-5 the high resolution spectrum reveals that the europium ion is in symmetry sites lower than axial. The spectroscopy of the Eu³⁺ ion in various crystal field environments is well known.¹¹⁻¹³ The thermoluminescence of Eu³⁺ below 170°K is very different from the thermoluminescence above 170°K (see Figs. 3, 4 and Table I). It is easy to identify these thermoluminescence spectra with the ⁵D₀ to ⁷F₁ transition (see Refs. 5-7). Since ⁵D₀ is a single level and cannot

be split, the group of three lines belongs to the splitting of ⁷F₁ in the crystal field. The Hamiltonian of this level with spin $S=1$ is given by:

$$\mathcal{H} = A / \{ 4S(S-1) [3S_z^2 - S(S+1) + \frac{1}{2}\eta(S_+^2 + S_-^2)] \} \quad (1)$$

or

$$\mathcal{H} = A / \{ 4 [3S_z^2 + \frac{1}{2}\eta(S_+^2 + S_-^2)] \}, \quad \text{for } S=1. \quad (2)$$

The constants A and η describe the crystal field splitting. Formally the Hamiltonian has the same form as the one conventionally used to describe the pure nuclear quadrupole interaction,¹⁴ η describes the discrepancy from axial symmetry. For $\eta=0$ there are two degenerate energy levels corresponding to the states $|\pm 1\rangle$ and single state $|0\rangle$. This is the case of axial symmetry. For $\eta \neq 0$ the three levels are split. The coefficient η changes from 0 to 1 in the Hamiltonian (1), where the z direction is defined as the direction of the largest component of the second derivative of the electric potential which interacts with the quadrupole moment of the electronic wavefunction of

TABLE I. Thermoluminescence data on CdF₂:Eu (⁵D₀ to ⁷F₁ transition).

Data below 170°K		Data above 170°K	
(Å)	(cm ⁻¹)	(Å)	(cm ⁻¹)
5936	16 846	5930	16 863
5921	16 889	5905	16 934
5906.5	16 930	5890	16 977

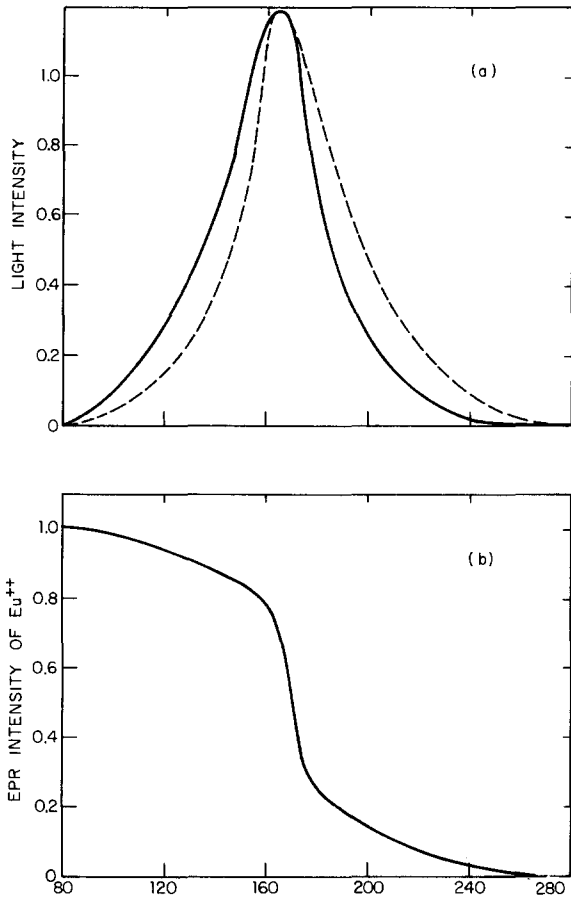


FIG. 2. (a) The solid line represents the total intensity of the thermoluminescence as a function of the temperature for CdF₂:Eu(0.02%); the dotted line represents the thermoluminescence of CdF₂:Eu(0.07%) as a function of the temperature. (b) The EPR intensity of x-irradiated CdF₂:Eu(0.02%) is plotted vs temperature.

Eu³⁺ in the ⁷F₁ group of levels:

$$E_{1,2} = \frac{3}{4A(1 \pm \eta/3)}, \quad (3)$$

$$A = \frac{2}{3(E_1 + E_2)}; \quad \eta = 3 \frac{E_1 - E_2}{E_1 + E_2},$$

where E_1 and E_2 are the energy gaps according to Fig. 6.

The fluorescence data shown in Fig. 5 of CaF₂:Eu are different from Kingsley and Prener¹³ (see Table XIII). They reported data in which it is clear that the symmetry of the Eu³⁺ ion is very close to axial symmetry. The reason for the discrepancy is probably that the charge compensation, which depends on the crystal growing conditions, is quite different. We are able to detect neatly the following groups of lines: ⁵D₀-⁷F₁, ⁵D₀-⁷F₂, ⁵D₀-⁷F₃, and ⁵D₀-⁷F₄ (see Figs. 6 and 7). The results are tabulated in Table II and shown in Fig. 7. The two spectra of thermoluminescence can be seen in the fluorescence spectrum [Fig. 6(b)].

The advantages of thermoluminescence in spectroscopy of ions in the crystal field are obvious. For comparison we also examine the fluorescence spectrum of double doped CdF₂ (with Eu and Na): see Table II. In this case we obtained only the ⁵D₀-⁷F₁ transition which was very intense. This spectrum also consists of three lines and indicates symmetry sites lower than axial. The parameters of A and η [see Eq. (3)] are:

(a) Low-temperature thermoluminescence $A = 83.3$ cm⁻¹; $\eta = 0.792$.

(b) High-temperature thermoluminescence $A = -104.7$ cm⁻¹; $\eta = 0.678$.

(c) Double doped CdF₂ fluorescence $A = -36.7$ cm⁻¹; $\eta = 0.678$.

B. Optical Absorption and EPR of Semiconducting CdF₂:Eu

If CdF₂:Eu is baked in Cd vapor the insulating CdF₂ ($\zeta \sim 10^9 \Omega \cdot \text{cm}$) is converted to a semiconductor ($\zeta \sim 500 \Omega \cdot \text{cm}$). Since Eu³⁺ is a much deeper trap than the shallow traps such as Cd, Sm, Y, Yb, the resistivity is two or three orders of magnitude larger for this semiconductor. Figure 8 shows the near-infrared absorption spectrum of converted CdF₂:Eu. Two broad absorption peaks are found peaked at 2650 cm⁻¹ (0.33 eV) and 1100 cm⁻¹ (0.136 eV). These peaks do not exist in the unconverted sample. The absorption in the visible region reveals the

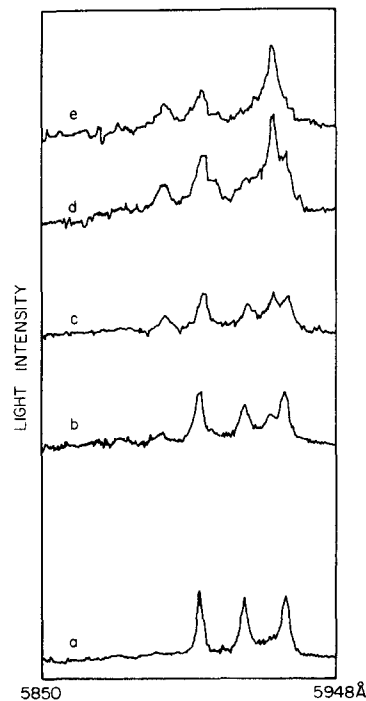


FIG. 3. Thermoluminescence spectra of CdF₂:Eu(0.02%) as a function of the temperature; trace a as the lowest temperature range; b, c, and d are spectra at intermediate temperatures; e the highest temperature range.

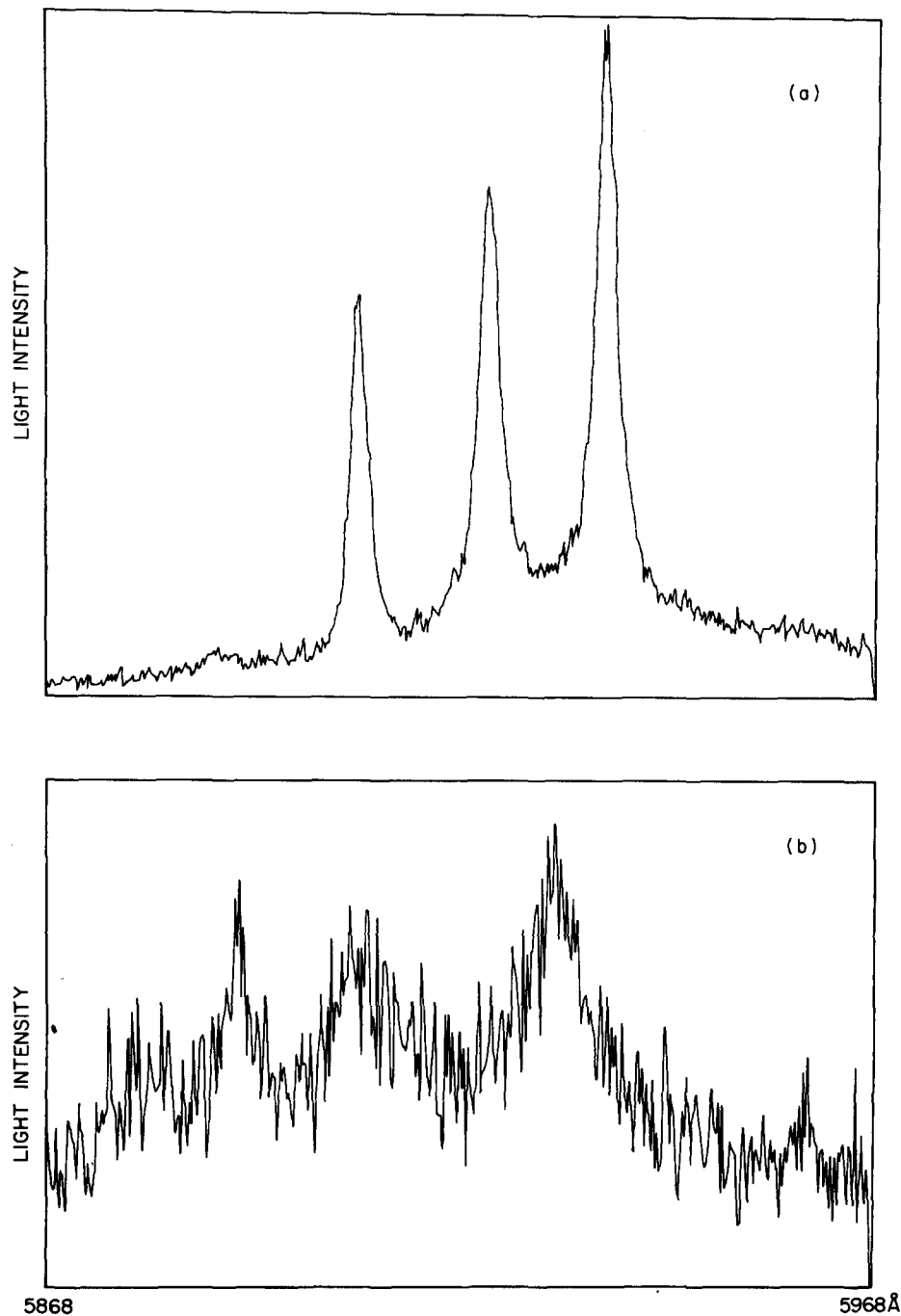


FIG. 4. (a) Thermoluminescence spectrum of $\text{CdF}_2:\text{Eu}$ (0.07%) below 170°K ; these lines are assigned to the ${}^6D_0-{}^7F_1$ transition. (b) Same as (a) above 170°K .

existence of Eu^{2+} . The $337\text{-m}\mu$ peak is identical with previously reported results.⁶

The converted $\text{CdF}_2:\text{Eu}$ is studied by EPR technique. The spectrum at 77°K confirms the existence of Eu^{2+} . The g factor, the crystal field parameters and the hyperfine structure are identical to those of the x-irradiated sample. We studied the EPR spectrum at room temperature, 77 , and 4.2°K . The intensity of Eu^{2+} spectrum at 77°K is 4.5 times greater than the spectrum at room temperature. In both cases the

intensity of the spectrum of Eu^{2+} is compared to the intensity of Mn^{2+} at low power to avoid saturation effects. At room temperature in addition to the normal Eu^{2+} spectrum a broad line is observed. This broad line is observed only when the magnetic field is at a certain angle, so that the seven Zeeman split energy gaps of the ${}^8S_{7/2}$ ground state are approximately equal.¹⁵ As in the case of Gd^{3+} in CdF_2 , when converted, this eight resonance is interpreted as an average line due to the exchange interaction between the con-

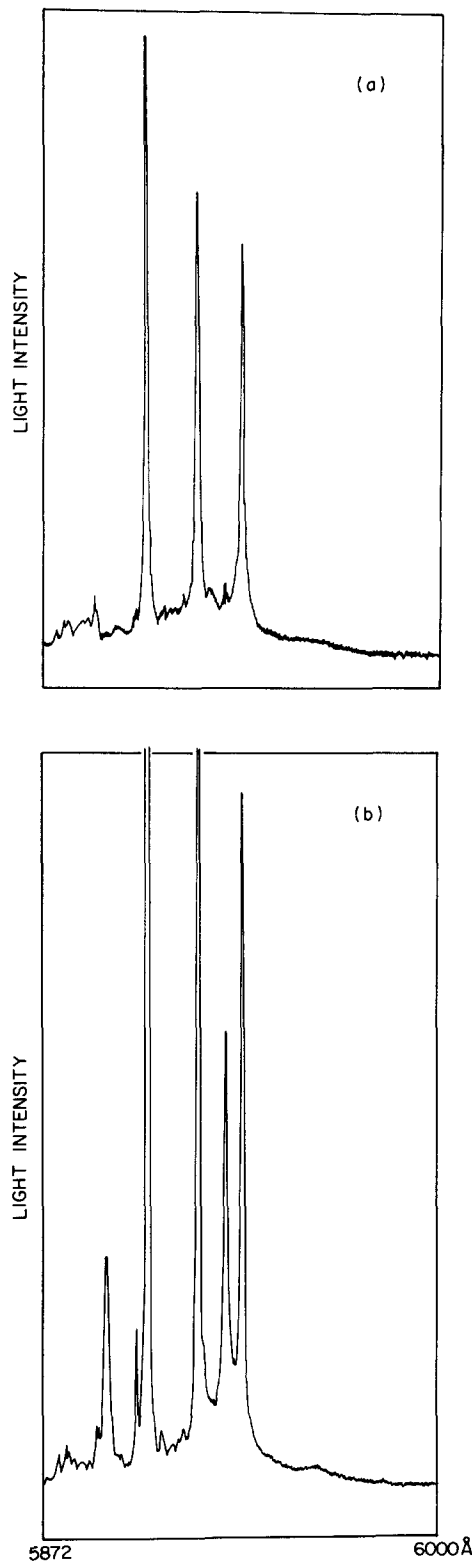


FIG. 5. (a) Fluorescence spectrum of CdF₂:Eu(0.07%). The three intense lines are assigned to the ⁵D₀-⁷F₁ transition (77°K). (b) Fluorescence spectrum of CdF₂:Eu(0.02%); the superposition of the two kinds of spectra is shown ((77°K).

duction electron and Eu²⁺. This broad signal disappears when the sample is cooled down to 77°K and the intensity of Eu²⁺ is increased. No difference is observed between the Eu²⁺ spectrum at 4.2 and 77°K.

The width of the "eighth resonance" line at room temperature close to the "magic angle" (when the energy levels are equally spaced) is changing according to the following table:

$\theta(^{\circ})$	0	2	3	4	6
$\Delta f(g)$	120	200	240	320	550.

TABLE II. Fluorescence data of CdF₂:Eu at 77°K.

(Å)	(cm ⁻¹)	(Å)	(cm ⁻¹)
(1) ⁵ D ₀ to ⁷ F ₁ transition			
5936	16 846	5931	16 860
5921	16 889	5903	16 940
5906	16 931	5891	16 975
(2) ⁵ D ₀ to ⁷ F ₂ transition			
6185	16 168		
6176	16 192		
6163	16 226		
6148	16 265		
6145	16 273		
(3) ⁵ D ₀ to ⁷ F ₃ transition			
6520	15 337		
6518	15 342		
6515	15 349		
6459	15 397		
6492	15 404		
6486	15 418		
6471	15 454		
(4) ⁵ D ₀ to ⁷ F ₄ transition			
6927	14 436		
6915	14 461		
6907	14 478		
6905.5	14 481		
6895	14 503	(two overlapping lines)	
6843	14 613		
6825	14 652		
6816	14 671		
Fluorescence data of CdF ₂ :Eu:Na at 77°K			
(1) ⁵ D ₀ to ⁷ F ₁ transition			
(Å)	(cm ⁻¹)		
5907	16 929		
5904	16 938		
5896	16 961		

The crystal is rotated in the (100) plane relative to the magnetic field.

It is difficult in the case of europium to estimate the exchange interaction because of the anisotropic hyperfine interaction with the two nuclear isotopes (^{151}Eu and ^{153}Eu).

III. EXPERIMENTAL TECHNIQUE

The CdF_2 single crystals used in this work were grown in graphite crucibles by use of Brodgener-Stockbarger technique.¹⁶⁻¹⁹ The CdF_2 powder was obtained from the General Electric Chemical Products Plant. The pure powder was first purified by repeated growth of single crystals. After each growth the top end was cut off and the remainder was ground up to be used as initial powder for the next growth. After purification the dopant was added to the pure powder and thus regrown. As grown, the samples were highly insulating. A Pyrex tube was cleaned and baked under vacuum at 500°C for 2 h. The doped sample and a piece of cadmium metal were placed in the tube so

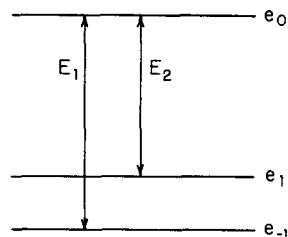


FIG. 6. Scheme of the crystal field split of 7F_1 level.

that they were physically separated. The tube was sealed and placed in a furnace. The crystal was heated at about 600°C for half an hour and removed from the furnace while hot.

Electron spin resonance data were taken with Varian V-4500 35-Gc/sec spectrometer. A special attachment has been built⁹ to allow both x-ray irradiation and collection of EPR data, keeping the sample at 77°K . Figure 9 shows the attachment which consists of a quartz Dewar with two suprasil quartz windows, 0.020 in. thick each. X-ray exposures are made with a molybdenum x-ray tube powered by a General Electric supply operated at 50 kV and 20 mA. The bottom part of the 35-Gc/sec cavity and the cold finger are supported by springs. The sample is at the level of the window during x-ray exposure. After the irradiation, the cavity and the wave guide with the iris is screwed up into the bottom part of the cavity. They are pushed down so the sample sits on the middle of the 8-in. pole of the Harvey-Wells Nuclear Corp. magnet. The sample temperature is measured by a copper-constantan thermocouple (made from 30-gauge wire) with reference junction in icewater. The thermocouple junction is pressed to the bottom part

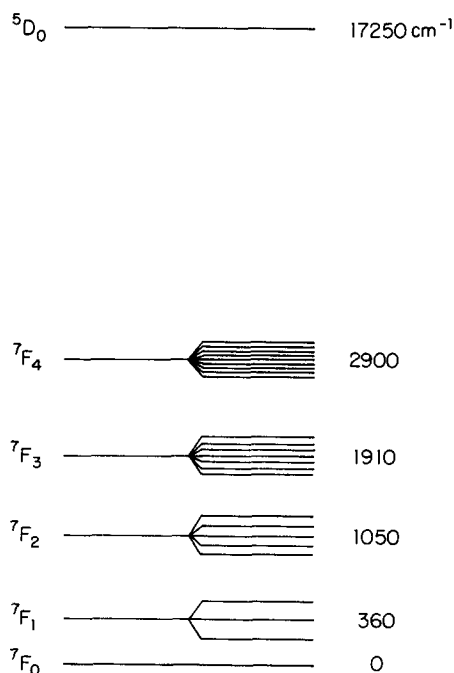


FIG. 7. Scheme of the electronic energy levels of Eu^{3+} .

of the cavity, as close to the sample as possible. The static magnetic field is measured by a free precession NMR signal with spin-echo apparatus.

The absorption measurements in the visible region are done in a Cary 14 spectrometer and the near-infrared region in a Cary-White 90 spectrometer. A liquid nitrogen Dewar with KBr windows is used for this purpose.

The high-resolution spectrum of thermoluminescence as well as the fluorescence spectrum is taken with Jarrel-Ash 1-m spectrometer (model 78-420). The excitation of the fluorescence spectrum is done by uv mercury lamp (General Electric Co., Hendersonville, N. C.), model B-H6 (900 W).

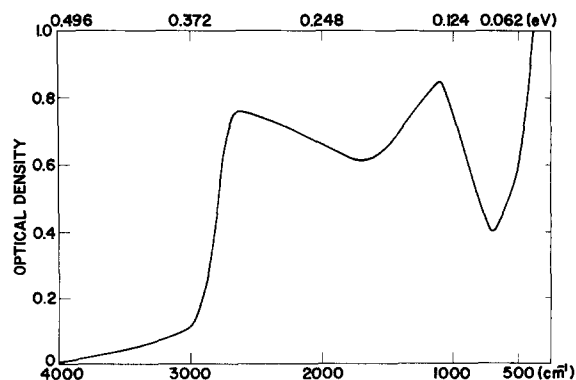


FIG. 8. Near-infrared absorption of semiconducting $\text{CdF}_2:\text{Eu}(0.07\%)$.

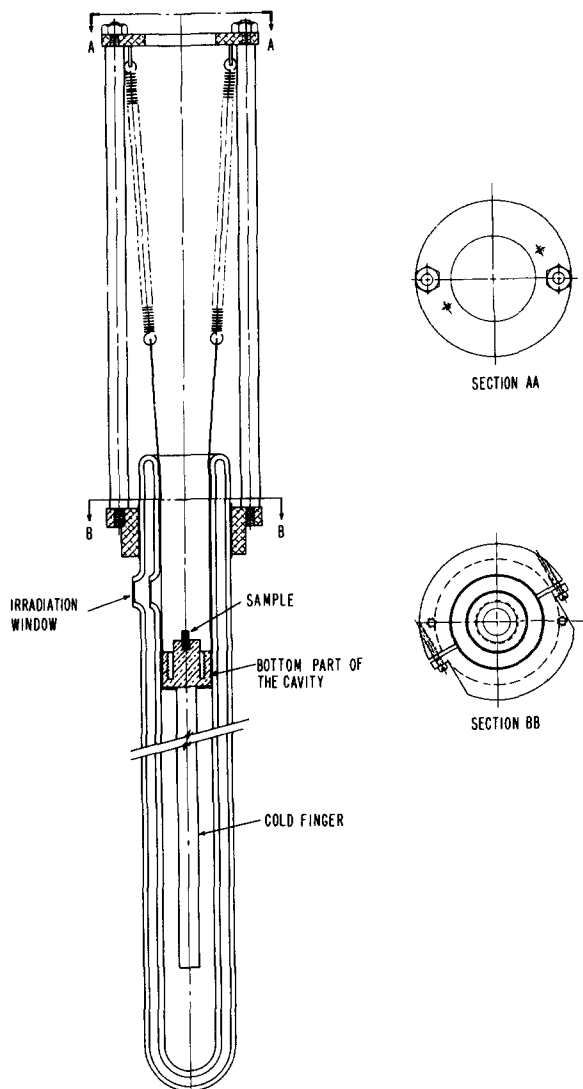


FIG. 9. Liquid nitrogen quartz Dewar with the bottom part of the cavity supported by springs. This attachment allows us to irradiate the sample at 77°K and measure the EPR spectra without heating the sample. The Dewar is used also to measure the thermoluminescence spectra.

The dimensions of the sample used in the fluorescence and thermoluminescence are: 10×10×6 mm; for EPR experiments—6×1.6×1.6 mm; the thickness of the sample used in optical absorption was about 1 mm.

IV. DISCUSSION

Irradiation damage (x-ray irradiation at 77°K) is almost not manifested in pure CdF₂ or CdF₂ doped with "shallow traps" rare earth. When Eu ions are not present the thermoluminescence intensity is about three orders of magnitude less and is probably not connected with the specific rare earth. The thermoluminescence of Eu³⁺ in CdF₂ is quite strong and it has the feature that is identical to the luminescence

spectrum excited by uv source. This proves the assumption that Eu³⁺ is a deep electron trap in the CdF₂ host. The shallow electron traps (rare earth) repel the electron mainly on the 5s shell of the cadmium. The EPR of Eu²⁺ due to the x-ray irradiation at 77°K (Fig. 1) in cubic or almost cubic sites proves that the electron excited from the valence fluorine band is excited into the cadmium conduction band, which lies at least 6 eV higher than the valence band, and trapped into the Eu³⁺, thus converting it into Eu²⁺. As shown in Fig. 2, the electron (or the hole center) is mobile and thermally activated at 170°K. As a result a recombination occurs^{9,10} and one is able to observe the spectroscopy of Eu³⁺. The experimental results show that there are two kinds of low symmetry sites for Eu³⁺. It is logical to assume that interstitial fluorines or cadmium vacancies cause this low symmetry; Interstitial fluorine in ⟨210⟩ position from the europium (C_{1h} symmetry) will split the three levels of ⁷F₁.

It is clear from Figs. 3, 4, and 7 that if the sample is more doped, the intensity of one kind of spectrum is increased relative to the intensity of the second kind. This suggests that this second kind of spectrum is related to a constant amount of some defect (Cd²⁺ vacancy, for instance), which does not depend on the amount of doping. It is striking that the Eu²⁺ is in cubic symmetry but the thermoluminescence spectrum is a low symmetry one. A possible explanation is that the level ⁸S_{7/2} belongs to an S-site ion where the crystal field splitting affects it only in higher orders, whereas the amount of splitting for the ⁷F₁ is much greater (of the order of 100 cm⁻¹). We wish to compare this result with the zero field splitting of Gd³⁺ in CaF₂ in the ground (⁸S_{7/2}) and an excited state (⁶P_{7/2}). From the cubic EPR spectrum the zero field splitting is 0.149 cm⁻¹; however, the splitting of ⁶P_{7/2} level from fluorescence measurement of Mokovsky²⁰ is 56.6 cm⁻¹.

On the basis of optical absorption and EPR data, we wish to propose the following model for the semi-conducting CdF₂:Eu; this model is consistent with the experimental results obtained for the insulating CdF₂:Eu. The ground state of the conduction electron is the Eu²⁺, which merely means that the low-lying energy level represents the europium impurity site (trap). The first excited state which is 0.136 eV above the ground state is 12 times degenerate; it represents the 12 cadmium nearest-neighbor sites at ⟨110⟩ type of direction from the europium impurity. At 77°K the ground state (Eu²⁺) is four times more populated (Boltzmann factor) than at room temperature. This property is exhibited in the increase of the intensity of EPR of the Eu²⁺ at 77°K relative to the intensity at room temperature. The increase in intensity is relative to the Mn²⁺ signal. The conduction band consists of more distant cadmium sites relative to the rare earth in 0.33 eV above the ground state.

* This work was supported in part by the Joint Services Electronics Program (U.S. Army, U.S. Navy, and U.S. Air Force) under Contract No. N00014-67-A-0298-0006 and by the Division of Engineering and Applied Physics, Harvard University.

† Present address: Microwave Division, The Racah Institute of Physics, The Hebrew University of Jerusalem, Israel.

¹ J. D. Kingsley and J. S. Prener, *Phys. Rev. Letters* **8**, 315 (1962).

² Z. J. Kiss and P. N. Yocom, *J. Chem. Phys.* **41**, 1511 (1964).

³ P. F. Weller, *Inorg. Chem.* **4**, 1545, (1965).

⁴ W. M. Latimer, *Oxidation Potentials* (Prentice-Hall, Englewood Cliffs, N.J., 1938), pp. 293-301.

⁵ P. Eisenberger and P. S. Pershan, *Phys. Rev.* **167**, 292 (1968).

⁶ F. Trautweiler, F. Moser, R. P. Khosla, *J. Phys. Chem. Solids* **29**, 1869 (1968).

⁷ H. J. Glazer and D. Geist, *Z. Naturforsch.* **20a**, 842 (1965).

⁸ W. Hayes and J. W. Twidell, *Proc. Phys. Soc. (London)* **29**, 1295 (1962); *Paramagnetic Resonance*, edited by W. Low (Academic, New York, 1963), Vol. 1., p. 163.

⁹ A. Tzalmona and P. S. Pershan, *Appl. Phys. Letters* **13**, 262 (1968); *Phys. Rev.* **182**, 906, (1969).

¹⁰ J. L. Mertz and P. S. Pershan, *Phys. Rev.* **162**, 217, 235

(1967); *Optical Properties of Ions in Crystals*, edited by H. M. Crosswhite and H. W. Moos (Interscience, New York, 1967), p. 117; J. L. Mertz, Ph.D. thesis, submitted to Harvard University, December, 1966.

¹¹ N. C. Chang and J. B. Gruber, *J. Chem. Phys.* **41**, 3227, (1964).

¹² O. J. Sovers and T. Yoshioka, *J. Chem. Phys.* **49**, 4945 (1968).

¹³ J. D. Kingsley and J. S. Prener, *Phys. Rev.* **126**, 458 (1962).

¹⁴ T. P. Das and E. L. Kahn, *Nuclear Quadrupole Resonance Spectroscopy* (Academic, New York, 1958), Chap. 1.

¹⁵ W. Low, *Phys. Rev.* **105**, 265 (1958).

¹⁶ D. C. Stockberger, *J. Opt. Soc. Am.* **39**, 731 (1949).

¹⁷ I. V. Stepanov and P. P. Fofilov in *Growth of Crystals*, edited by A. V. Shubnikov and N. N. Sheftal (Consultants Bureau, New York, 1959), Vol. 1. Chap. IV.

¹⁸ H. M. Baker, W. Hayes, and D. A. Jones, *Proc. Phys. Soc. (London)* **73**, 942, (1959).

¹⁹ H. Guggenheim, *J. Appl. Phys.* **34**, 2482, (1963).

²⁰ J. Makovsky, *Phys. Quantum Electronics Conference*, edited by P. L. Kelley, B. Lax, and P. E. Tannenwald (McGraw-Hill, New York, 1966); *J. Chem. Phys.* **46**, 390 (1967).

THE JOURNAL OF CHEMICAL PHYSICS VOLUME 55, NUMBER 10 15 NOVEMBER 1971

Kinetic Salt Effects on the Aquation Reaction of the Azidopentaaquochromium (III) Ion and Predictions of the Mayer Theory

A. INDELLI AND R. DE SANTIS

Istituto di Chimica Analitica ed Elettrochimica, Via Risorgimento, 35—Pisa, Italy

(Received 2 June 1971)

The rate of the reaction of aquation of the azidopentaaquochromium(III) ion has been measured at two different concentrations of hydrogen ion in the presence of a number of salts. The values of k_1 and k_0 of the equation

$$k_{obs} = k_1[H^+] + k_0 + k_{-1}[H^+]^{-1} + k_{-2}[H^+]^{-2}$$

were calculated and both show positive salt effects and obey the Olson-Simonson rule. Calculations performed using the Mayer theory in the approximation "DHLL+B₂" have shown that at high dilution both these effects can be rationalized using appropriate values of the distances of closest approach. The possibility of using this form of the Mayer theory for extrapolation purposes is suggested. The use of different distances of closest approach for different pairs of ions does not lead to any inconsistency.

Kinetic salt effects on reactions involving ions of the same sign cannot, in general, be satisfactorily interpreted on the basis of the simple Brønsted-Debye theory.¹ For reactions between anions the rate does not depend upon the ionic strength, I , but upon the nature and concentration of the cations, whereas for reactions between cations it is the concentration of the anions which is important.² This can not be rationalized in terms of the Brønsted-Debye theory, even with the assumption of the formation of reactive ion pairs.³ Moreover, salt effects are sometimes observed also for unimolecular reactions or for reactions between an ion and a neutral molecule,⁴ and these cannot be interpreted on the basis of the simple Brønsted-Debye theory but require the assumption of a specific ionic interaction.⁵ Quantitative studies on this subject are rather scarce.⁶ Moreover, the instances of salt effects in reactions between cations which are found in the literature are usually complicated by the formation of complexes of the reactants with the added salts and are not suitable for a

study in terms of an electrostatic theory. Therefore we considered it useful to measure the salt effects in the aquation of the azidopentaaquochromium ion which offers interesting opportunities. In fact this reaction has been studied by Swaddle and King⁷ who found that the rate in a wide range of H⁺ concentration and at an ionic strength $I = 1.0M$, could be expressed by the equation

$$V = k_1[Cr][H^+] + k_0[Cr] + k_{-1}[Cr]/[H^+] + k_{-2}[Cr]/[H^+]^2, \quad (1)$$

where $[Cr]$ is the concentration of the complex. The first rate constant, k_1 , corresponds to a reaction between two cations, whereas the second, k_0 , corresponds to a unimolecular reaction, or, possibly, to a reaction between a cation and a neutral solvent molecule. Under suitable conditions it is possible to neglect the contributions of the third and fourth terms. The Mayer theory,⁸ even in a very crude form, appears to be able